Algeria

# Influence of rest time on the structural and surface properties of macroporous silicon

K.R. Chebouki <sup>a,\*</sup>, L. Remache <sup>a</sup>, F. Saker <sup>a</sup>, L. Grine <sup>b</sup>, S. Çolak <sup>c,d</sup>, S. Çakar <sup>e,f</sup> <sup>a</sup> Laboratory of Materials and System Structure and their Reliability, Oum El Bouaghi University, Oum El Bouaghi, 04000, Algeria <sup>b</sup> Laboratory of Study of Electronic Materials for Medical Applications (LEMEAMED), University of Frère Mentouri Constantine 1, Constantine, 25000,

This study investigates the effect of rest time (Tr) during the electrochemical anodization of n-type (100) silicon in hydrofluoric acid-based solutions, with the objective of tuning the morphological, structural, and surface properties of macroporous silicon (MPSi). Anodization was carried out at a constant current density of 10 mA/cm<sup>2</sup> under white light illumination for 20 minutes. Rest periods of 0, 20, 40, 60, and 80 seconds were introduced between etching intervals to examine their influence on pore development. Morphological analysis using Field-Emission Scanning Electron Microscopy (FE-SEM) revealed that Tr significantly affects pore shape and distribution. The sample with a 40-second rest time exhibited the most regular and circular pores, with the highest porosity (72%) and largest average pore diameter (~5.05 μm). Beyond this optimal point, longer rest times led to irregular morphologies and reduced porosity. Structural characterization via X-ray Diffraction (XRD) confirmed the preservation of the silicon crystal structure, with minor variations in crystallite size. Contact angle measurements demonstrated that surface wettability is also Tr-dependent, with the lowest contact angle (~43°) observed at Tr = 40 s, indicating enhanced hydrophilicity. The improvement in pore uniformity and surface properties is attributed to the enhanced removal of hydrogen bubbles and better electrolyte renewal during rest periods. These results underscore the importance of temporal modulation in anodization processes and highlight rest time as a critical parameter for optimizing MPSi for applications in sensors, biomedical interfaces, and optoelectronic devices.

(Received June 11, 2025; Accepted September 9, 2025)

*Keywords:* Macroporous silicon, Electrochemical anodization, Rest time, Porosity, Pore size

## 1. Introduction

Semiconductor materials have attracted significant interest over the past decades due to their exceptional electrical, optical, and photonic properties, making them indispensable in a wide range of modern technologies, including microelectronics, photonics, and chemical sensing [1, 2].

<sup>&</sup>lt;sup>c</sup> Department of Chemical and Chemical Processing Technologies, Çaycuma Food and Agriculture Vocational School,, Zonguldak, 67100, Türkiye

<sup>&</sup>lt;sup>d</sup> Science and Technology Reseach and Application Center (ARTMER), Zonguldak Bülent Ecevit University, Zonguldak, 67100, Türkiye

<sup>&</sup>lt;sup>e</sup> Chemistry Department, Art and Science Faculty, Zonguldak Bülent Ecevit University, Zonguldak, 67100, Türkiye

<sup>&</sup>lt;sup>f</sup>Biomaterials, Energy, Photocatalysis, Enzyme Technology, Nano Advanced Materials, Additive Manufacturing, Environmental Applications and Sustainability Research Development Group (BIOENAMS, Sakarya University, Sakarya, 54050, Türkiye

<sup>\*</sup> Corresponding author: Cheboukirime@gmail.com https://doi.org/10.15251/DJNB.2025.203.1113

Among these, porous silicon (PSi) has emerged as a particularly versatile platform owing to its high specific surface area, tunable nanostructure, low processing cost, and compatibility with conventional silicon microfabrication techniques [3-5]. These attributes have enabled its integration into numerous applications such as biosensing, photodetectors, drug delivery systems, and energy storage devices [5, 6]. According to IUPAC classification, porous materials are divided into three categories based on pore diameter: microporous (<2 nm), mesoporous (2–50 nm), and macroporous (>50 nm) [7]. In particular, macroporous silicon (MPSi) has gained considerable attention due to its ability to form deep, vertically aligned pores with large diameters and well-defined geometries, making it highly suitable for applications requiring efficient molecular transport or surface functionalization [8]. The structural and morphological characteristics of MPSi including pore size, shape, distribution, porosity, and grain structure are highly sensitive to the electrochemical etching conditions used during fabrication [9-11].

Several key anodization parameters influence the final morphology of MPSi layers. These include the current density, which governs the silicon dissolution rate and pore formation kinetics [12]; The etching time, which controls pore depth; the composition and viscosity of the electrolyte (typically hydrofluoric acid with ethanol or surfactants) [13-15]; and the illumination conditions [16], which are critical for n-type silicon substrates to generate minority carriers. Additionally, the resistivity and crystallographic orientation of the silicon wafer (e.g., (100) vs (111)) significantly affect pore alignment and ordering [17-19]. Beyond traditional static parameters, dynamic modulation methods based on periodic current interruption has garnered increasing interest for their ability to enhance pore morphology and layer uniformity in MPSi. This approach introduces rest periods (Tr) during the anodization process, during which the current is temporarily interrupted. These pauses allow hydrogen gas bubbles to escape from the pore tips and enable the diffusion of fresh HF electrolyte to the etching front, reducing surface passivation and concentration gradients [1, 20]. While conventional etching parameters have been extensively studied, the effects of temporal modulation strategies like Tr remain relatively underexplored. Nonetheless, Tr has shown significant potential to influence local etching dynamics by facilitating surface stress relaxation, promoting by-product removal, and improving electrolyte accessibility. These mechanisms collectively contribute to better pore propagation, increased structural ordering, and enhanced overall integrity of the porous layer without altering the global anodization duration or current density [20, 21].

A comparative study by Razali et al. demonstrated the distinct advantages of the iPEC method over traditional direct current anodization (DCPEC). Their findings revealed that while DCPEC produced square-shaped pores with approximately 40% porosity, the iPEC technique generated a mix of square and cross-shaped pores with significantly higher porosity (~52%) and improved surface regularity [20].

These findings underscore the essential influence of both static (chemical/electrical) and dynamic (temporal/modulated) elements in shaping the morphology and functionality of macroporous silicon. The capacity to enhance these characteristics provides an efficient method for developing MPSi layers with specific characteristics for photonic, biological and sensing applications.

The originality of this work lies in the implementation of significantly prolonged rest times (Tr) during the electrochemical anodization of silicon, reaching up to 80 seconds—well beyond the millisecond-scale pauses reported in earlier studies. Previous research has primarily focused on tuning static parameters such as current density, etching time, and electrolyte composition, or on introducing brief pulsed interruptions to enhance pore formation. For instance, Amran et al. [21] and Naderi et al. [1] employed pulse anodization with delay times restricted to a few milliseconds. In contrast, our study adopts a temporal modulation approach by incorporating extended rest periods, aiming to improve etching uniformity and structural properties. We specifically examine the influence of Tr on the morphological and surface characteristics of macroporous silicon (MPSi) formed on n-type (100) silicon in HF-based solutions. The etching process includes intermittent pauses introduced without altering the overall anodization duration or current density. The resulting samples were characterized in terms of structural and morphological properties using X-ray diffraction (XRD) and Field-Emission Scanning Electron Microscopy (FE-SEM), respectively. Surface wettability was evaluated through contact angle measurements. The

overall objective is to elucidate the influence of rest time on the development and characteristics of macroporous silicon matrices.

## 2. Experimental

### 2.1. Preparation of MPSi

The porous silicon layers were fabricated using an electrochemical etching method on n-type silicon substrates with a (100) crystallographic orientation and a resistivity range of 1–20  $\Omega$ ·cm. The electrolyte used was a mixture of hydrofluoric acid (HF), ethanol, and hydrogen peroxide (H<sub>2</sub>O<sub>2</sub>) in a ratio of 1:2:1. The etching process was performed at room temperature in a Teflon cell to protect against the corrosive effects of HF. A lamp positioned 30 cm from the cell provided the necessary illumination to generate minority carriers during etching. Prior to the etching, the silicon samples were immersed in a 2% HF solution to remove the native oxide layer. Electrochemical anodization was carried out using a Keithley power supply, with a constant current density of 10 mA/cm<sup>2</sup> applied for 20 minutes (Figure 1).

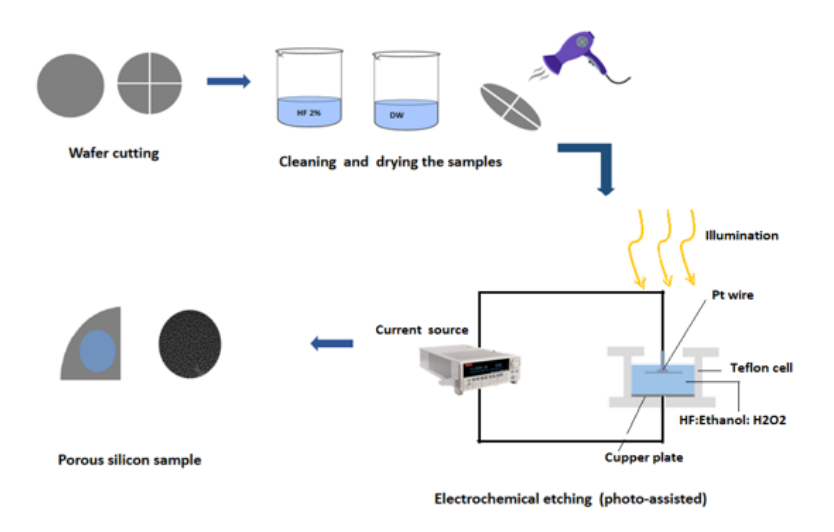


Fig. 1. The process involved in fabricating silicon with a macroporous structure.

## 2.2. Introduction of rest time

During electrochemical anodization, the chemical reactions are accompanied by the release of hydrogen gas bubbles, which adversely affect both the etching rate and the stability of the electrolyte. As the reactions progress within the pores, the hydrofluoric acid is gradually consumed, leading to a local decrease in its concentration and, consequently, a reduction in the overall etching efficiency. Moreover, the accumulation of hydrogen bubbles inside the pores further impedes the etching process, resulting in the formation of shallower pores [22].

To overcome these limitations, a discontinuous current approach was adopted, alternating between an active etching period (T) and a rest time (Tr). This strategy facilitates the evacuation of hydrogen bubbles and enhances the diffusion of fresh HF molecules toward the pore tips, thereby maintaining a relatively constant HF concentration near the silicon surface [23]. The rest period (Tr) corresponds to an electroless phase, during which no current is applied, while the active period (T) represents the anodization phase, during which a constant current density of 10 mA/cm² is maintained [1].

In this study, a pulsed anodization protocol was employed, consisting of three cycles. Each of the first two cycles comprised an active period (T) followed by a rest time (Tr). In contrast, the third cycle included only the active period (T), without a subsequent Tr, as illustrated in (Figure 2). This modulation scheme (T + Tr) repeated twice, followed by a final T was designed to promote

homogeneous pore propagation and improve pore morphology, without increasing the total anodization duration. To evaluate the effect of rest time on the structural and morphological properties of macroporous silicon, five samples were prepared using different Tr values: 0 s (reference), 20 s, 40 s, 60 s, and 80 s. After etching, all samples were rinsed in ethanol to remove residual species.

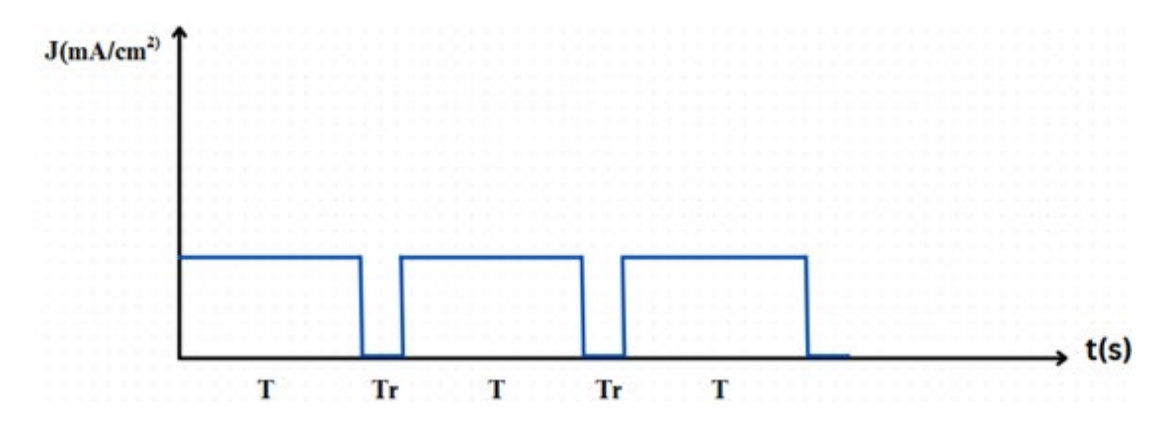


Fig. 2. Chronogram of the applied current density during the etching process.

### 2.3. Characterization

To investigate the surface morphology, the synthetized samples were examined using Field-Emission Scanning Electron Microscopy (FE-SEM, FEI ESEM Quanta 450 FEG). The pore morphology was further analyzed using ImageJ software. Structural characterization of the macroporous silicon (MPSi) was performed using X-ray diffraction (XRD) with a Panalytical Empyrean diffractometer, employing Cu K $\alpha$  radiation ( $\lambda$  = 1.5406 Å) at 45 kV and 40 mA, with a step size of 0.02°. The average crystallite size was estimated using the Scherrer equation. Surface wettability was evaluated by contact angle measurements, conducted using a Gaosuo 500X adjustable digital USB microscope in conjunction with the Gaosuo microscope software.

### 3. Results and discussion

# 3.1. Effect of the rest times on the pore morphology

Figure 3 presents the FE-SEM images of n-type porous silicon obtained by electrochemical anodization. The five images clearly demonstrate that the etching process is homogeneous across the entire analyzed surface. For the reference sample (a) (Tr = 0 s), the porosity is approximately 54%, and the pores exhibit a quadrilobed and interconnected morphology. In sample (b) (Tr = 20 s), the pore morphology evolves further, becoming more irregular and tending toward a circular shape, with a noticeable increase in both pore size and porosity. At Tr = 40 s sample (c), the pores adopt a well-defined circular morphology while remaining interconnected. The continued increase in pore size and porosity suggests enhanced stability of the anodization solution. The introduction of a rest time facilitates the removal of hydrogen bubbles from the pore tips and allows fresh hydrofluoric acid (HF) to reach and react with the silicon surface, thereby improving etching efficiency and increasing surface porosity, as reported in [21].

Moreover, Arman et al. [21] observed that during the rest period, the oxide layer formed on the silicon surface tends to dissolve. This results in the thinning of the barrier layer, which subsequently allows a higher current density during the next active etching phase. The disappearance of hydrogen bubbles also promotes homogeneous etching along all crystallographic directions (100, 010, and 001), thus favoring the formation of circular pores.

In sample (d) (Tr = 60 s), a reduction in pore size is observed, with the pores adopting a more triangular morphology. In sample (e) (Tr = 80 s), the pores regain a quadrilobed shape, but with more elongated lobes compared to those seen in the reference sample (Tr = 0 s).

These observations are consistent with prior studies on n-type porous silicon, which have shown that for (100) oriented silicon, the main pores tend to propagate in the  $\langle 100 \rangle$  direction, while lateral etching occurs along the  $\langle 010 \rangle$  and  $\langle 001 \rangle$  directions [24, 25]. Our results for Tr = 0 s and Tr = 20 s confirm this anisotropic behavior. However, at Tr = 40 s, lateral etching appears to proceed at an equal rate in all directions, resulting in the formation of more circular pores. The evolution of pore shape as a function of rest time is further illustrated in (Figure 4).

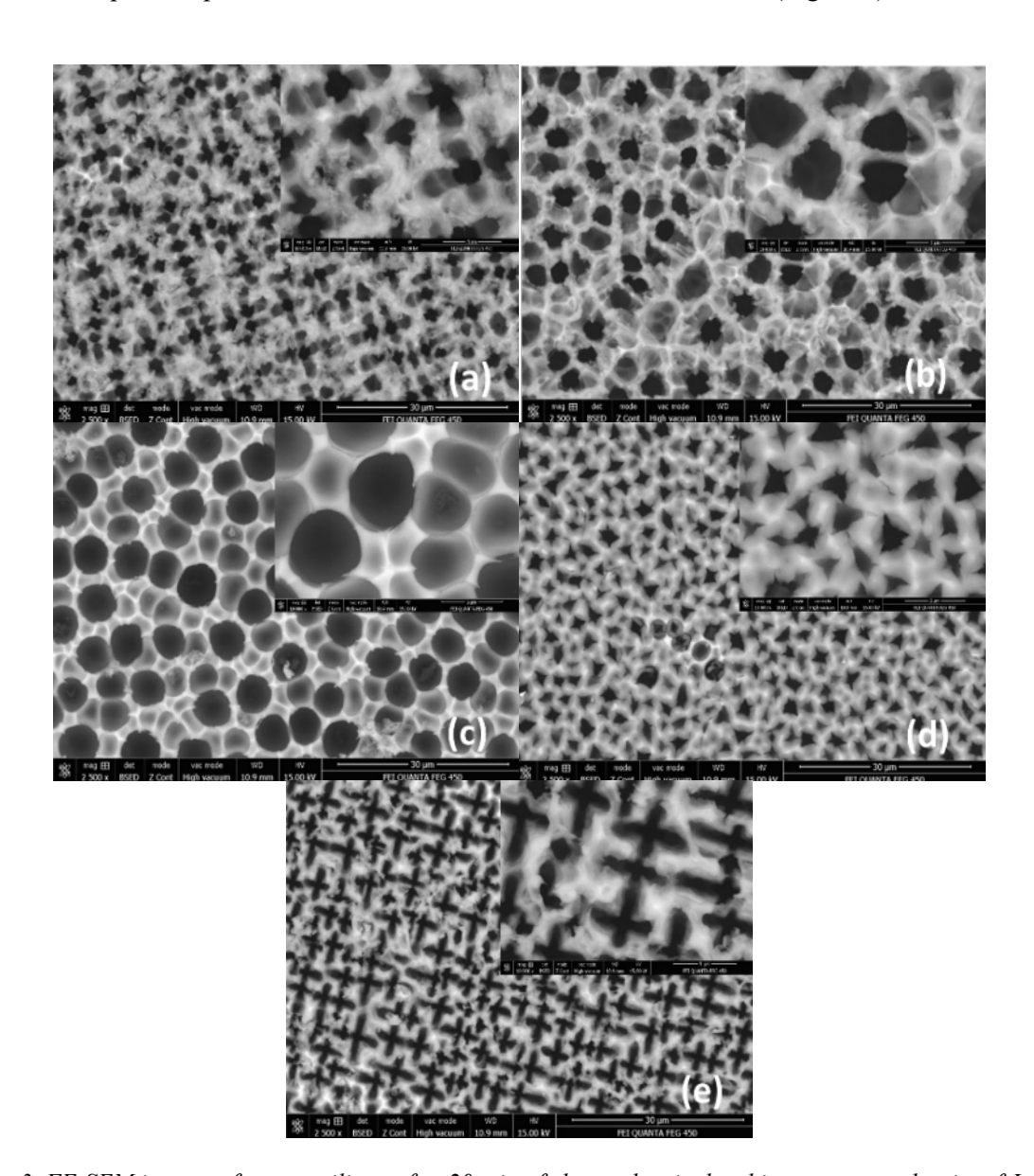


Fig. 3. FE-SEM images of porous silicon after 20 min of electrochemical etching at current density of J=10 mA/cm2 with different rest times (a) Tr=0s (reference), (b) Tr=20s, (c) Tr=40s, (d) Tr=60s, (e) Tr=80.

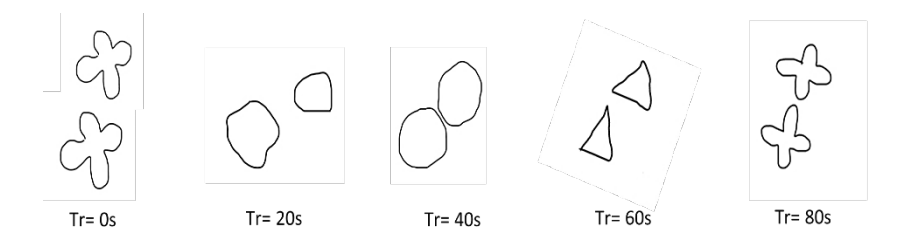


Fig. 4. The evolution of the pore shape in N-type macroporous silicon as a function of rest time.

# 3.2. Effect of rest time on porosity and average pore size

The porosity and average pore size of porous silicon are highly sensitive to several anodization parameters, including current density, etching duration, HF concentration, and illumination conditions [20]. In the present study, the impact of rest time (Tr) between successive etching intervals was specifically investigated. Quantitative analysis of SEM images using ImageJ software allowed for the estimation of porosity and average pore diameter as functions of Tr.

The results reveal that both porosity and pore size exhibit a nonlinear dependence on the rest time. An increase in Tr initially enhances both parameters, reaching a maximum at Tr=40~s, where the porosity peaks is 72% and the average pore diameter is 5.054  $\mu m$ . However, further increases in rest time led to a notable decline in both values, with Tr=60~s resulting in only 30% of porosity and an average pore diameter of 2.322  $\mu m$  (Figure 5a).

This trend is also reflected in the average pore size evolution (Figure 5b), which increases with moderate rest times but diminishes at higher values. This behavior suggests the presence of an optimal Tr that maximizes pore growth and structural development. Beyond this optimal value, the etching process becomes less efficient, likely due to excessive relaxation periods that alter the balance between electrochemical activity and chemical dissolution, leading to reduced pore propagation.

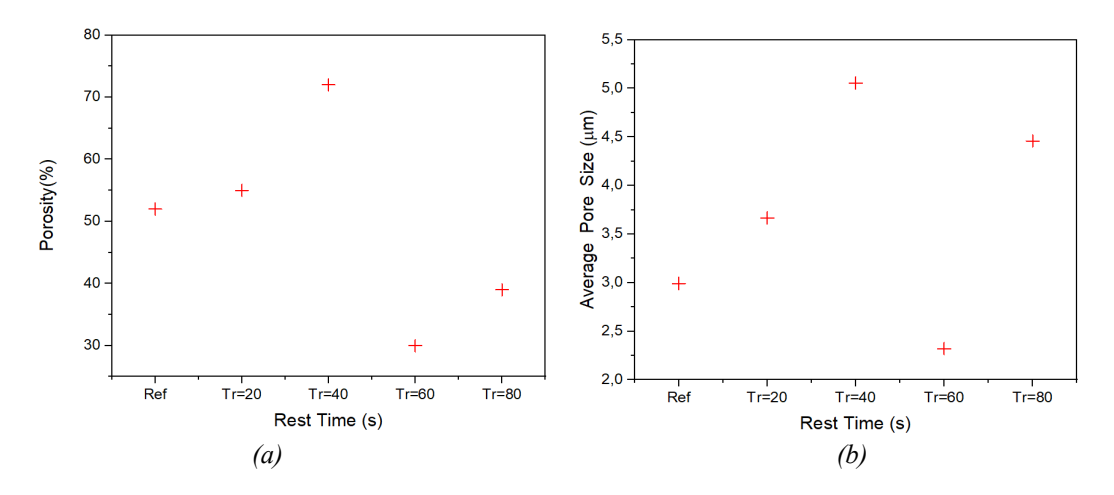


Fig. 5. (a) Porosity and (b) Average pore size as a function of rest time (Tr).

## 3.3. Effect of rest time on the structure of MPSi

The X-ray diffraction (XRD) results provide valuable insights into the crystallographic structure of electrochemically etched silicon samples as a function of rest time (Tr). The diffraction patterns exhibit two main peaks at  $2\theta = 69.2^{\circ}$  and  $2\theta = 69.4^{\circ}$ , corresponding to the (400) and (422) cubic planes of silicon, respectively, based on the JCPDS card No. 89–2955 [26]. The peak at  $2\theta = 69.2^{\circ}$  is notably more intense across all samples, in agreement with previously reported studies [12, 21].

The consistency of peak positions among all samples indicates that the anodization process does not significantly alter the underlying crystallographic orientation of the silicon substrate. However, a clear trend is observed in peak intensity (Figure 6). The reference sample (Tr = 0 s) exhibits the highest peak intensity, suggesting minimal structural alteration and a higher degree of crystallinity. As Tr increases, the intensity gradually decreases, which may be attributed to increased surface porosity and minor lattice distortions introduced during the etching process.

Peak broadening, characterized by the full width at half maximum (FWHM,  $\beta$ ), exhibits only slight variation across the different samples (Table 1). According to the Debye-Scherrer equation [27], a smaller  $\beta$  value corresponds to better crystallinity and larger crystallite sizes. The calculated crystallite sizes show only minor differences between samples, confirming that the etching process with varying Tr values has limited impact on the overall crystal structure but may introduce surface-level modifications.

$$D = \frac{k\lambda}{\beta\cos\theta} \tag{1}$$

D: The diameter of the particles.

k: The shape constant, its value is about 0.9.

 $\lambda$ : The wavelength of the incident X-rays.

 $\beta$ : The (FWHM) full width at half maximum, and observed at the Bragg diffraction angle ( $\theta$ ).

 $\theta$ : Bragg angle.

The crystallite size (D) values obtained from XRD analysis exhibit slight variations across the different rest times (Tr). The reference sample (Tr = 0 s) presents an average crystallite size of 11.03 nm, while samples etched with Tr = 20 s and Tr = 40 s show increased values of 13.60 nm and 11.03 nm, respectively. This trend suggests that shorter rest times may favor the preservation or growth of larger crystallites, possibly due to more stable etching conditions. In contrast, longer rest times could promote minor structural reorganization at the nanoscale, leading to subtle reductions in crystallite size.

Overall, the XRD analysis confirms that electrochemical etching with varying Tr does not significantly alter the bulk crystal structure of silicon but does affect peak intensity and crystallite size, indicating surface-level modifications. The observed changes highlight the importance of achieving a balance between anodic and electroless etching phases. These findings suggest that optimizing the rest time (Tr) is a critical parameter for tuning the microstructural properties of porous silicon and enhancing its suitability for sensor applications [1].

Table 1. Summary of peak positions in  $2\theta$ ,  $\beta$ , crystallite size (D), and average crystallite size (Dmoy).

Sample	20	β	Height (cnt)	D	$D_{moy}$	$D_{moy}$
	(°)	(°)		(Å)	(A°)	(nm)
(REF)	69,21047	0,0936	4177107	117,47	110,28	11,028
	69,41379	0,0575	2218036	103,09		
tr=20s	69,19096	0,0624	4057936	117,45	136,055	13,605
	69,38857	0,0487	2458689	154,66		
tr=40s	69,18696	0,0936	3322315	117,44	110,27	11,027
	69,36211	0,0605	1747810	103,1		
tr=60s	69,17722	0,0936	3371058	117,44	110,27	11,027
	69,38823	0,0588	1843320	103,1		
tr=80s	69,21866	0,0936	4060359	117,46	110,335	11,033
	69,41454	0,0513	2433939	103,21		

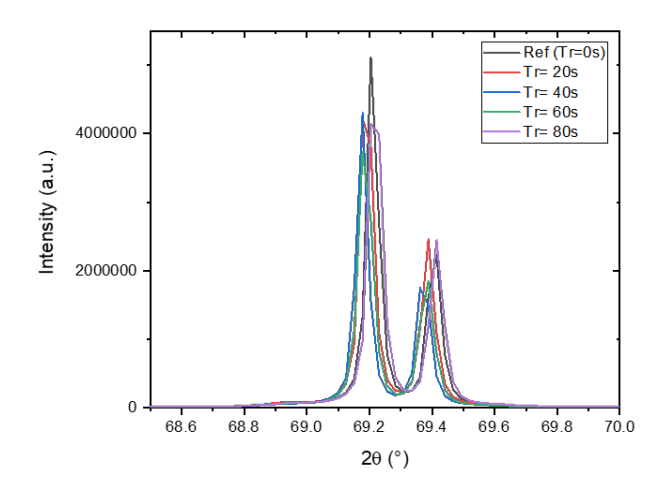


Fig. 6. XRD patterns of the sample etched by the electrochemical anodization with different rest times of MPSi.

# 3.4. Effect of rest time on the wettability properties of MPSi

In this section, we examine the wettability properties of macroporous silicon (MPSi), focusing on its hydrophilic or hydrophobic behavior as a function of rest time (Tr), using contact angle (CA) measurements. The contact angles were measured under ambient conditions. A 5  $\mu$ L droplet of distilled water was deposited on the surface of each sample, and the average contact angle was determined by taking multiple measurements at different locations (Figure 7).

The results show that rest time significantly affects the wettability of MPSi. This influence is evident in the non-linear variation of the contact angle with Tr (Figure 8). For all samples, the contact angle remains below  $90^{\circ}$ , indicating that the surfaces exhibit hydrophilic behavior. As the rest time increases, the contact angle generally decreases, reaching a minimum of  $43^{\circ}$  at Tr = 40 s, before increasing again for longer rest times.

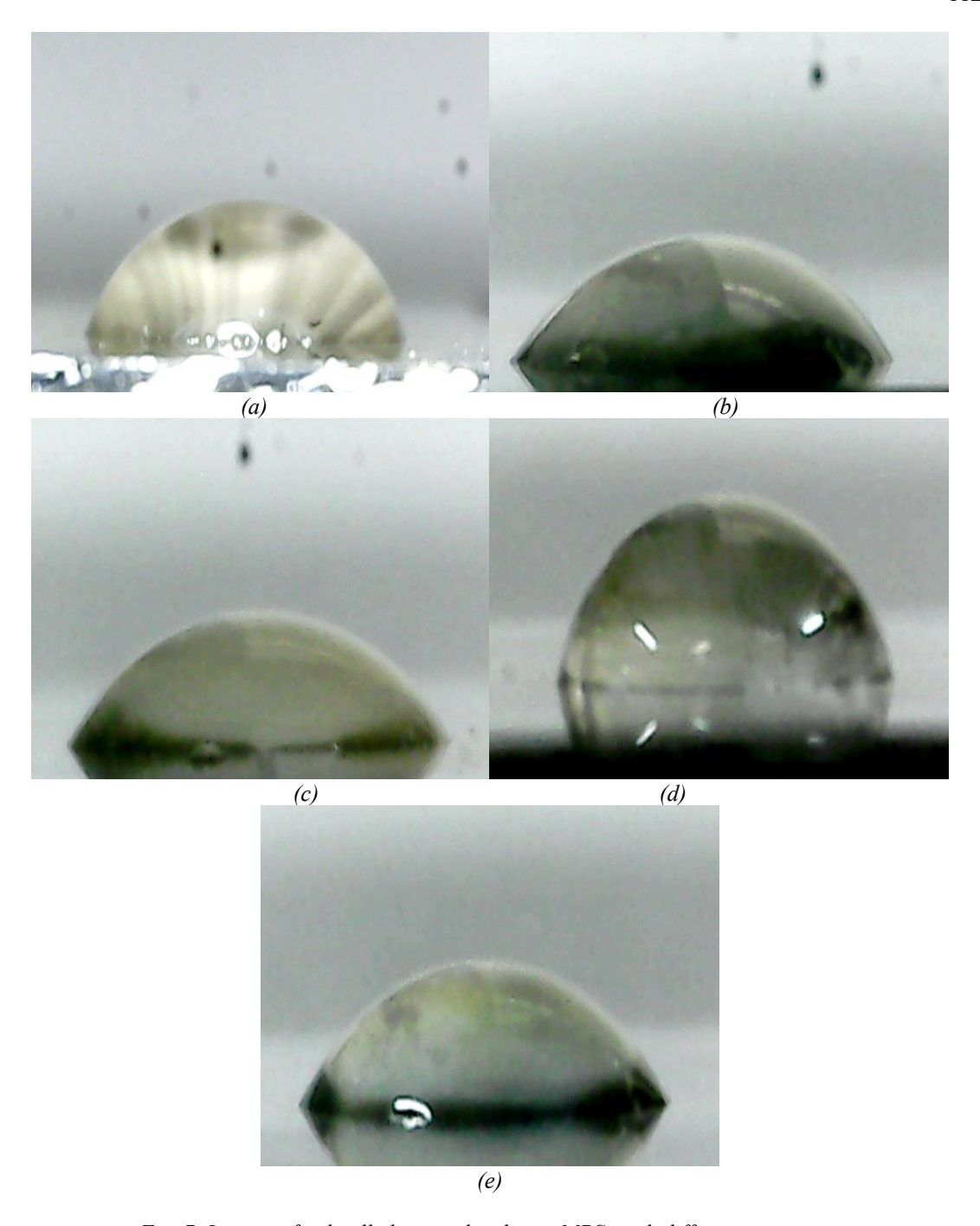


Fig. 7. Images of a distilled water droplet on MPSi with different rest times.

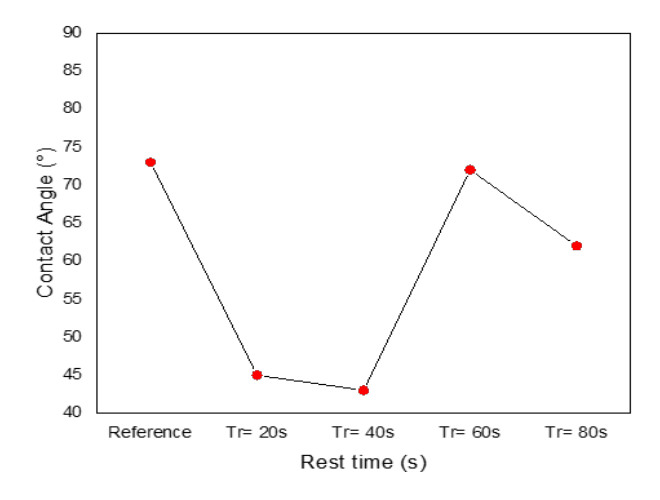


Fig. 8. Contact angle (°) as function of rest time(s) of MPSi.

This trend can be explained by the influence of pore structure on surface wetting. At moderate Tr values, the increase in porosity and pore diameter enhances the effective surface area, promoting better water spreading and stronger capillary effects, thus increasing hydrophilicity. In contrast, at longer rest times, the reduction in pore size and porosity leads to lower surface roughness and reduced capillarity, making the surface less hydrophilic [28].

These findings are in good agreement with those reported by Belorus et al., who showed that the wettability of porous silicon strongly depends on both surface morphology and the composition of functional groups. Specifically, they demonstrated that porous Si fabricated under optimized conditions exhibited a minimum contact angle of 43°, indicating maximum hydrophilicity, while deviations from these conditions led to increased hydrophobicity due to changes in surface structure and chemistry [29].

Therefore, optimizing Tr provides a valuable tool for modulating the surface energy and tailoring the wettability of MPSi, which is a key requirement in applications such as biosensing, microfluidics, and drug delivery systems.

### 4. Conclusion

Macroporous silicon (MPSi) was successfully fabricated via electrochemical anodization. The introduction of rest time (Tr) during the process proved to be a crucial parameter for stabilizing the electrolyte and modulating the structural and surface properties of the resulting porous silicon. SEM analysis demonstrated that Tr strongly influences both pore size and morphology, with moderate Tr values leading to increased porosity and pore diameter, followed by a decline beyond a certain threshold. XRD analysis confirmed that the crystalline structure of silicon remains largely preserved, with only minor variations in crystallite size. Contact angle measurements further revealed that Tr significantly affects the surface wettability of MPSi, in direct correlation with the evolution of pore structure. These findings highlight the importance of rest time in tailoring the morphology and functional properties of MPSi, making it a promising strategy for the optimization of materials intended for applications in optoelectronics, biomedical engineering, chemical sensing, and biosensing platforms.

# Acknowledgments

This work partially was supported by the Scientific Research Projects Commission of Zonguldak Bülent Ecevit University (Project number: 2022-72118496-02 and 2024-72118496-07).

### References

- [1] N. Naderi, M. Hashim, T. Amran, Superlattices and Microstructures, vol. 51, no. 5, pp. 626-634, 2012; https://doi.org/10.1016/j.spmi.2012.03.010
- [2] F. Ameen, M. Younus, G. Ali, Chalcogenide Letters, vol. 21, no. 4, pp. 343-354, 2024; https://doi.org/10.15251/CL.2024.214.343
- [3] O. Kuntyi, G. Zozulya, M. Shepida, Advances in Materials Science and Engineering, vol. 2022, no. 1, p. 1482877, 2022; <a href="https://doi.org/10.1155/2022/1482877">https://doi.org/10.1155/2022/1482877</a>
- [4] P. Kumar, P. Huber, Journal of Nanomaterials, vol. 2007, no. 1, p. 089718, 2007; https://doi.org/10.1155/2007/89718
- [5] C. A. Betty, Recent Pat Nanotechnol, vol. 2, no. 2, pp. 128-36, 2008; https://doi.org/10.2174/187221008784534514
- [6] A. S. Lenshin et al., Coatings, vol. 13, no. 2, p. 385, 2023; https://doi.org/10.3390/coatings13020385
- [7] T. R. Somo, M. J. Hato, K. D. Modibane, Advanced functional porous materials: from macro to nano scale lengths: Springer, 2021, pp. 87-111; <a href="https://doi.org/10.1007/978-3-030-85397-6">https://doi.org/10.1007/978-3-030-85397-6</a> 4
- [8] P. Granitzer, K. Rumpf, Materials, vol. 3, no. 2, pp. 943-998, 2010; https://doi.org/10.3390/ma3020943
- [9] A. Langner, F. Müller, U. Gösele, Molecular-and nano-tubes, pp. 431-460, 2011; https://doi.org/10.1007/978-1-4419-9443-1 13
- [10] H. Ouyang, M. Christophersen, P. M. Fauchet, Physica Status Solidi A, vol. 202, no. 8, pp. 1396-1401, 2005; https://doi.org/10.1002/pssa.200461112
- [11] C. R. Miranda, M. R. Baldan, A. F. Beloto, N. G. Ferreira, Journal of the Brazilian Chemical Society, vol. 19, pp. 769-774, 2008; <a href="https://doi.org/10.1590/S0103-50532008000400022">https://doi.org/10.1590/S0103-50532008000400022</a>
- [12] A. J. Fulton, V. O. Kollath, K. Karan, Y. Shi, Journal of Applied Physics, vol. 124, no. 9, 2018; <a href="https://doi.org/10.1063/1.5041373">https://doi.org/10.1063/1.5041373</a>
- [13] T. Defforge, M. Diatta, D. Valente, F. Tran-Van, G. Gautier, Journal of The Electrochemical Society, vol. 160, no. 4, p. H247, 2013; <a href="https://doi.org/10.1149/2.013306jes">https://doi.org/10.1149/2.013306jes</a>
- [14] K. Kordás, J. Remes, S. Beke, T. Hu, S. Leppävuori, Applied Surface Science, vol. 178, no. 1, pp. 190-193, 2001/07/02/ 2001; https://doi.org/10.1016/S0169-4332(01)00310-5
- [15] A. A. Abbas, S. J. Hasan, I. M. Abdulmajeed, S. Q. Hazaa, Iraqi Journal of Applied Physics, vol. 20, no. 1, 2024.
- [16] C. Tsai et al., Journal of Electronic Materials, vol. 21, no. 10, pp. 995-1000, 1992/10/01 1992; https://doi.org/10.1007/BF02684209
- [17] N. I. Rusli, M. S. Z. Abidin, B. Astuti, N. K. Ali, A. M. Hashim, 2012 International Conference on Enabling Science and Nanotechnology, 2012: IEEE, pp. 1-2; <a href="https://doi.org/10.1109/ESciNano.2012.6149705">https://doi.org/10.1109/ESciNano.2012.6149705</a>
- [18] M. Christophersen, J. Carstensen, S. Rönnebeck, C. Jäger, W. Jäger, H. Föll, Journal of The Electrochemical Society, vol. 148, no. 6, p. E267, 2001/06/01 2001; <a href="https://doi.org/10.1149/1.1369378">https://doi.org/10.1149/1.1369378</a>
- [19] J. Zhang, F. Zhang, M. Ma, Z. Liu, Micromachines, vol. 16, no. 2, p. 154, 2025; https://doi.org/10.3390/mi16020154
- [20] N. Razali et al., Acta Physica Polonica: A, vol. 135, no. 4, 2019; https://doi.org/10.12693/APhysPolA.135.697
- [21] T. Amran, M. Hashim, N. Ali, H. Yazid, R. Adnan, Physica B: Condensed Matter, vol. 407, no. 23, pp. 4540-4544, 2012; <a href="https://doi.org/10.1016/j.physb.2012.08.008">https://doi.org/10.1016/j.physb.2012.08.008</a>
- [22] N. K. Ali, M. R. Hashim, A. A. Aziz, Solid-State Electronics, vol. 52, no. 7, pp. 1071-1074, 2008/07/01/2008; <a href="https://doi.org/10.1016/j.sse.2008.03.010">https://doi.org/10.1016/j.sse.2008.03.010</a>
- [23] N. Ali, M. Hashim, A. A. Aziz, Electrochemical and Solid-State Letters, vol. 12, no. 3, p. D11, 2008; <a href="https://doi.org/10.1149/1.3049861">https://doi.org/10.1149/1.3049861</a>

- [24] P. C. Searson, J. M. Macaulay, F. M. Ross, Journal of Applied Physics, vol. 72, no. 1, pp. 253-258, 1992; <a href="https://doi.org/10.1063/1.352123">https://doi.org/10.1063/1.352123</a>
- [25] S. Rönnebeck, J. Carstensen, S. Ottow, H. Föll, Electrochemical and solid-state letters, vol. 2, no. 3, p. 126, 1998; <a href="https://doi.org/10.1149/1.1390756">https://doi.org/10.1149/1.1390756</a>
- [26] M. Husham, Z. Hassan, A. M. Selman, The European Physical Journal Applied Physics, vol. 74, no. 1, p. 10101, 2016; <a href="https://doi.org/10.1051/epjap/2016150414">https://doi.org/10.1051/epjap/2016150414</a>
- [27] F. Saker, L. Remache, D. Belfennache, K. Chebouki, R. Yekhlef, Chalcogenide Letters, vol. 22, no. 2, 2025; <a href="https://doi.org/10.15251/CL.2025.222.151">https://doi.org/10.15251/CL.2025.222.151</a>
- [28] P. Formentín, L. F. Marsal, Nanomaterials, vol. 11, no. 3, p. 670, 2021; <a href="https://doi.org/10.3390/nano11030670">https://doi.org/10.3390/nano11030670</a>
- [29] A. Belorus, Y. Bukina, A. Pastukhov, D. Stebko, Y. M. Spivak, V. Moshnikov, Journal of Physics: Conference Series, 2017, vol. 929, no. 1: IOP Publishing, p. 012051; https://doi.org/10.1088/1742-6596/929/1/012051